Available online at www.sciencedirect.com

SciVerse ScienceDirect

Ceramics International 39 (2013) 8207–8212

CERAMICS INTERNATIONAL

www.elsevier.com/locate/ceramint

# Effect of $La_2O_3$ addition on crystallization and properties of $Li_2O$–$Al_2O_3$–$SiO_2$ glass-ceramics

Ping Lu, Yong Zheng, Jinshu Cheng, Dongyun Guo*

*Green Building Materials and Manufacturing Engineering Research Center (Ministry of Education), Wuhan University of Technology, Wuhan 430070, China*

Received 2 March 2013; received in revised form 27 March 2013; accepted 1 April 2013
Available online 9 April 2013

**Abstract**

La-doped $Li_2O$–$Al_2O_3$–$SiO_2$ (LAS) glass-ceramics were prepared by solid phase reaction. Their crystallization, morphologies and properties were investigated. The crystallization temperature of LAS glass-ceramics decreased due to the $La_2O_3$ addition. For the La-doped LAS glass, the $\beta$-quartz solid solution (s.s.) was initially formed, and then the $\beta$-quartz s.s. transformed to $\beta$-spodumene at higher temperature. The $La_2O_3$ addition played a role of network modifier in the LAS glass altering their network structure. With increasing the $La_2O_3$ content, the flexural strength decreased, and the thermal expansion coefficient increased.


*Keywords:* B. Surface; B. X-ray methods; C. Thermal expansion; D. Glass-ceramics

## 1. Introduction

Compositions based on the ternary $Li_2O$–$Al_2O_3$–$SiO_2$ (LAS) system are extensively applied in industry for glass-ceramic production because of their low expansion coefficient, high transparency and excellent thermal shock resistance [1–3]. Recently, much attention has been concentrated on the rare-earth-doped LAS glass-ceramics, which are composed of a glassy matrix with rare earth containing nanocrystals and act as active optical materials for photonic applications [4–10]. Dymnikov et al. [4] investigated the structure of luminescence centers of $Nd^{3+}$ in LAS glass-ceramics and revealed that $Nd^{3+}$ ions entered into $\beta$-spodumene ($Li_2O \cdot Al_2O_3 \cdot 4SiO_2$) structure. Zheng et al.[9] prepared the Y-doped LAS glass-ceramics and found that the main crystalline phase of Y-doped LAS glass-ceramics was $\beta$-spodumene, which was formed directly without the transformation from $\beta$-quartz solid solution (s.s.) to $\beta$-spodumene during the crystallization treatment. Hu et al.[10] prepared Ce-doped LAS glass and found that the transformation of glass to $\beta$-quartz s.s., and $\beta$-quartz s.s. to $\beta$-spodumene were accelerated by the addition of $CeO_2$. Their results indicated that the addition of 5 wt% $CeO_2$ serving as a flux also promotes crystallization.

In the present study, La-doped LAS glass-ceramics have been prepared, and the effect of $La_2O_3$ content on their crystallization, mechanical properties and thermal expansion coefficient was investigated.

## 2. Experimental

The raw materials were reagent-grade $SiO_2$, $Al_2O_3$, $Li_2CO_3$, $Na_2CO_3$, $KNO_3$, $Sb_2O_3$, $NH_4H_2PO_4$, MgO, $TiO_2$, $ZrO_2$, ZnO, $H_3BO_3$ and $La_2O_3$. The composition in wt% of the base LAS glass-ceramic was: $Li_2O$(4.1), $Al_2O_3$(22.0), $SiO_2$(63.2), ZnO(1.0), MgO(1.5), $TiO_2$(2.0), $ZrO_2$(2.0), $Na_2O$(0.6), $K_2O$(0.3), $B_2O_3$(1.0), $Sb_2O_3$(1.1) and $P_2O_5$(1.2). The doping content of $La_2O_3$, which based on the total amount of the LAS glass, varied from 0, 2.5, 5.0 to 7.5 wt% (denoted as LAS, La1, La2 and La3, respectively). The desired amounts of the raw materials were melted in an electric furnace at 1650 °C for 3 h until a bubble-free liquid was formed, and then the melt was cast in a pre-heated mold. At last, to obtain glass-ceramics, these samples were heat-treated at different temperatures as shown in Table 1.

Differential scanning calorimetry (DSC) analysis was carried out using the thermal analyzer (Netzsch STA449C). The measurements

*Corresponding author. Tel.: +86 27 8721 7492; fax: +86 27 8787 9468.
*E-mail address:* guodongyun@gmail.com (D. Guo).

0272-8842/$ - see front matter © 2013 Elsevier Ltd and Techna Group S.r.l. All rights reserved.
http://dx.doi.org/10.1016/j.ceramint.2013.04.004

Table 1
Heat-treatment of La-doped LAS glass-ceramics.

| | Nucleation | Crystallization | Appearance |
|---|---|---|---|
| LAS | 600 °C/2 h | 765 °C/2 h | Transparent |
| | 600 °C/2 h | 800 °C/2 h | Translucent |
| | 600 °C/2 h | 860 °C/2 h | White opaque |
| La1 | 570 °C/2 h | 740 °C/2 h | Transparent |
| | 570 °C/2 h | 770 °C/2 h | Translucent |
| | 570 °C/2 h | 840 °C/2 h | White opaque |
| La2 | 570 °C/2 h | 770 °C/2 h | Translucent |
| La3 | 570 °C/2 h | 770 °C/2 h | Translucent |

were performed with LAS and La1 glass powders in Pt crucible with $Al_2O_3$ as the reference material in the temperature between 20 °C and 1000 °C with a heating rate of 10 °C $min^{-1}$. The crystalline phases in the glass-ceramics were analyzed using an X-ray diffractometer (XRD, RIGAKU D/max-RB). The glass-ceramics were etched in an HF solution (5%) for 90 s, and then their morphologies were observed using a scanning electron microscopy (SEM, JSM-5610LV). Infrared spectra of the glass-ceramics were obtained using an infrared Fourier spectrometer (Nicolet170) in the range of 400–2000 $cm^{-1}$. Four-point bending was used to obtain flexural strength (modulus of rupture) of the glass-ceramics at room temperature. The coefficient of thermal expansion of the glass-ceramics was measured using a thermo-dilatometer (PEY) in the temperature ranging from 20 to 400 °C.

## 3. Results and discussion

### 3.1. Heat-treatment of LAS glass-ceramics

Fig. 1 shows the DSC curve of LAS glass. The glass transformation point ($T_g$) ranged from 590 to 600 °C. There were two exothermic peaks at around 809 °C and 863 °C, which corresponded to the crystallization and phase transformation. In order to choose an efficient nucleation temperature for LAS glass-ceramics, the LAS glass was heated at the nucleation temperature of 600 °C for 2 h and then heated at crystallization temperatures ($T_c$) 765, 800 and 860 °C for 2 h. The XRD results of LAS glass-ceramics are shown in Fig. 2. At $T_c$=765 °C, the main phase was β-quartz s.s. in the LAS glass-ceramics. With increasing $T_c$ to 800 °C, the β-quartz s.s. phase coexisted with the β-spodumene phase. At higher $T_c$ (860 °C), the peak intensity of β-spodumene phase increased. These results indicate that the phase transformation of glass to β-quartz s.s., and β-quartz s.s. to β-spodumene.

Fig. 3 depicts the morphologies of LAS glass-ceramics after HF solution(5%)-etching. At $T_c$=765 and 800 °C, the LAS glass-ceramics consisted of very small size grains and the grain size was about 100 nm. With increasing $T_c$, the grain size increased. The grain size of the LAS glass-ceramics heated at 860 °C was more than 500 nm, and it also became white opaque.

### 3.2. Heat-treatment of La-doped LAS glass-ceramics

Fig. 4 shows the DSC curve of La1 glass (2.5 wt% $La_2O_3$ addition). The glass transformation point ($T_g$) ranged from 539

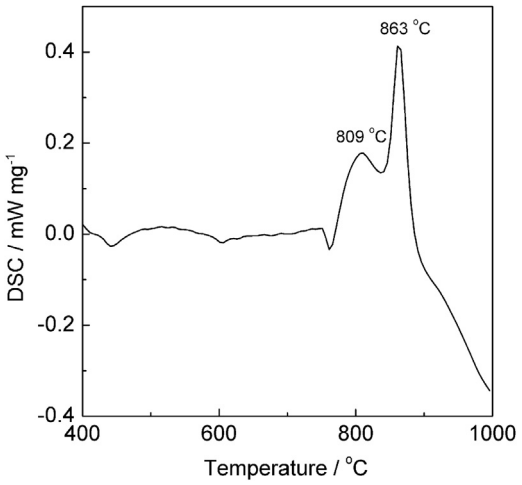


Fig. 1. Differential scanning calorimetry (DSC) analysis of LAS glass.

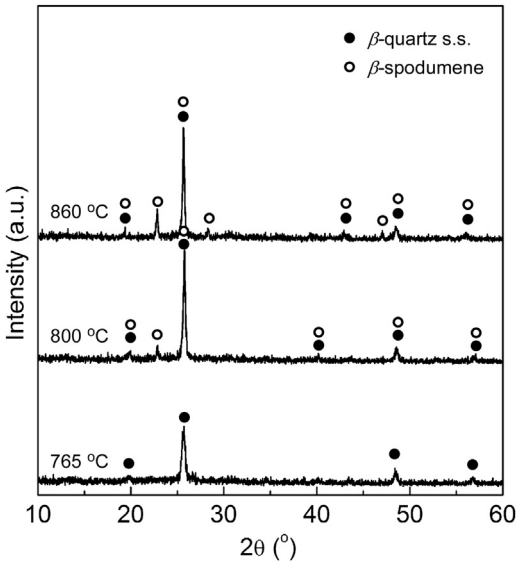


Fig. 2. XRD patterns of LAS glass-ceramics annealed at different temperatures.

to 575 °C. There were also two exothermic peaks at around 769 °C and 838 °C, which corresponded to the crystallization and phase transformation. Compared with the LAS glass, the temperatures of crystallization and phase transformation decreased. The La1 glass was heated at the nucleation temperature of 570 °C for 2 h and then heated at crystallization temperatures ($T_c$) 740, 770 and 840 °C for 2 h to obtain the glass-ceramics. The XRD results of La1 glass-ceramics are shown in Fig. 5. At $T_c$=765 °C, a broad scattering spectrum was observed, because small amount of β-quartz s.s. was formed in the La1 glass. As the glass sample was heated at higher $T_c$ of 770 °C, the peak intensity of β-quartz s.s. increased and the broad scattering spectrum disappeared. The β-quartz s.s. phase coexisted with the β-spodumene phase in the La1 glass-ceramics heated at 840 °C. For the La-doped LAS glass, the phase transformation of glass to β-quartz s.s.

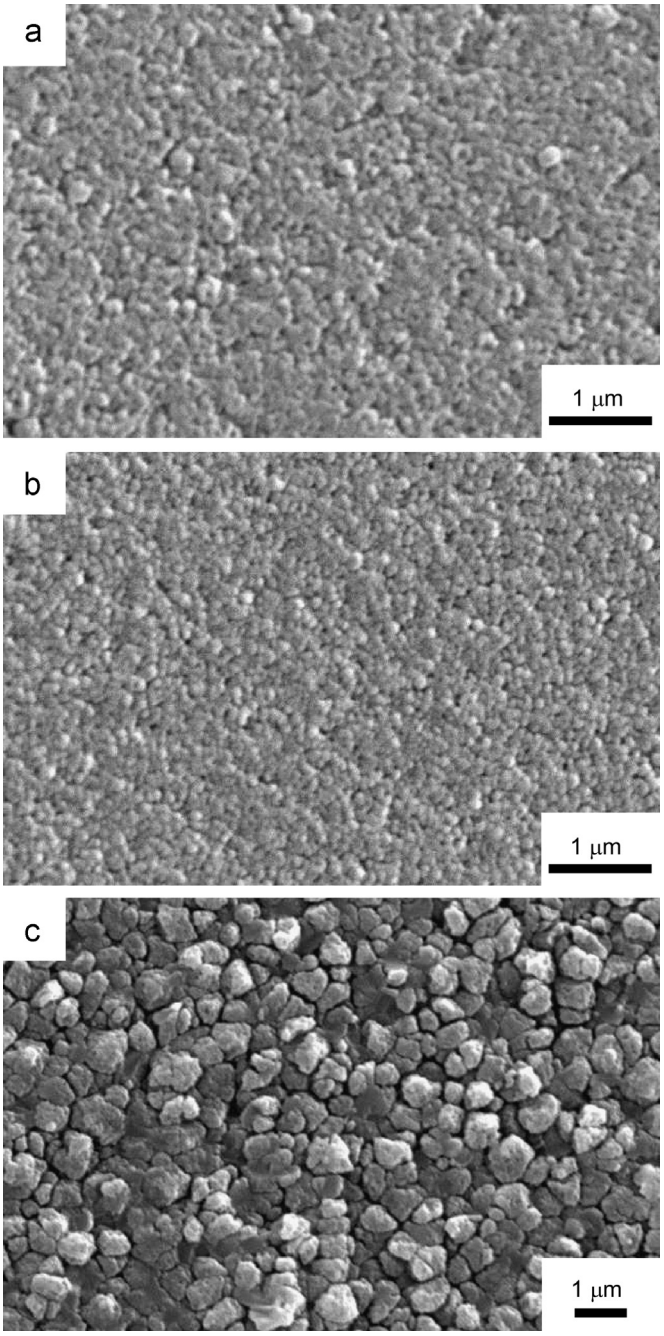


Fig. 3. Morphologies of LAS glass-ceramics annealed at different temperatures: (a) 765 °C, (b) 800 °C and (c) 860 °C.

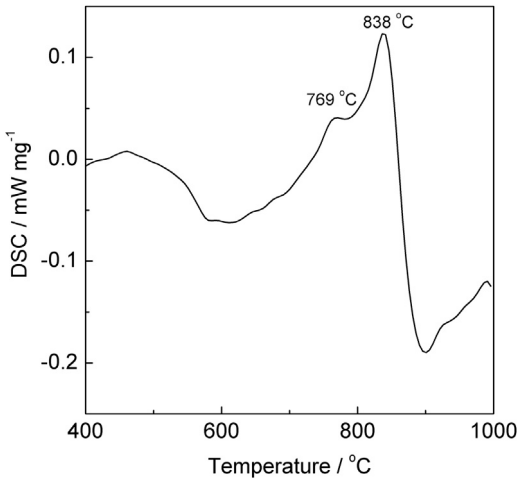


Fig. 4. Differential scanning calorimetry (DSC) analysis of La1 glass.

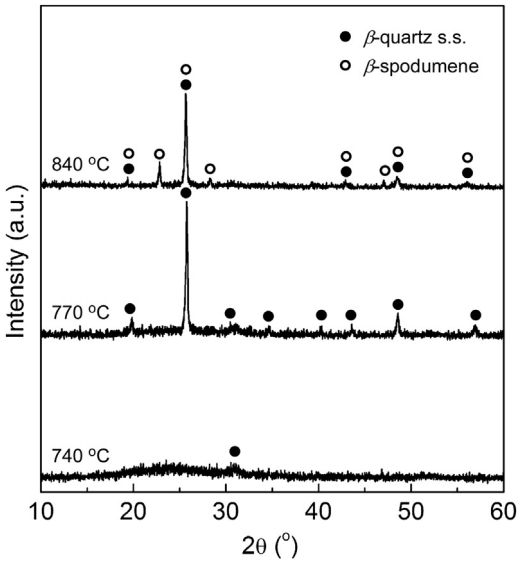


Fig. 5. XRD patterns of La1 glass-ceramics annealed at different temperatures.

firstly happened, and then the $\beta$-quartz s.s. transformed to $\beta$-spodumene, which coincided with the results of Ce-doped LAS glass-ceramics reported by Hu et al.[10]

Fig. 6 depicts the morphologies of La1 glass-ceramics after HF solution(5%)-etching. For the La1 glass-ceramics heated at $T_c$=740 °C, it was difficult to find the grains. At $T_c$=770 °C, the La1 glass-ceramics consisted of fine grains and the grain size was about 100 nm. With increasing $T_c$, the grain size increased. The grain size of the La1 glass-ceramics heated at 840 °C was about 1000 nm. With increasing $T_c$ from 740 to 840 °C, the La1 glass-ceramics changed from transparent to white opaque.

### 3.3. Properties of La-doped LAS glass-ceramics

Based on these results, to prepare the glass-ceramics samples for optical and mechanical properties measurements, the heat-treatment of the La-doped LAS glass-ceramics was selected. The LAS glass was heated at 600 °C for 2 h and then 800 °C for 2 h, while the La-doped glasses were heated at 570 °C for 2 h and then 770 °C for 2 h. Fig. 7 displays the XRD results of the glass-ceramics. The main phase of $\beta$-quartz s.s. was formed. With increasing $La_2O_3$ content, they showed almost the same XRD patterns. Fig. 8 demonstrates the morphologies of the glass-ceramics after HF solution(5%)-etching. For the LAS and La1 samples, they consisted of fine grains and the grain size was about

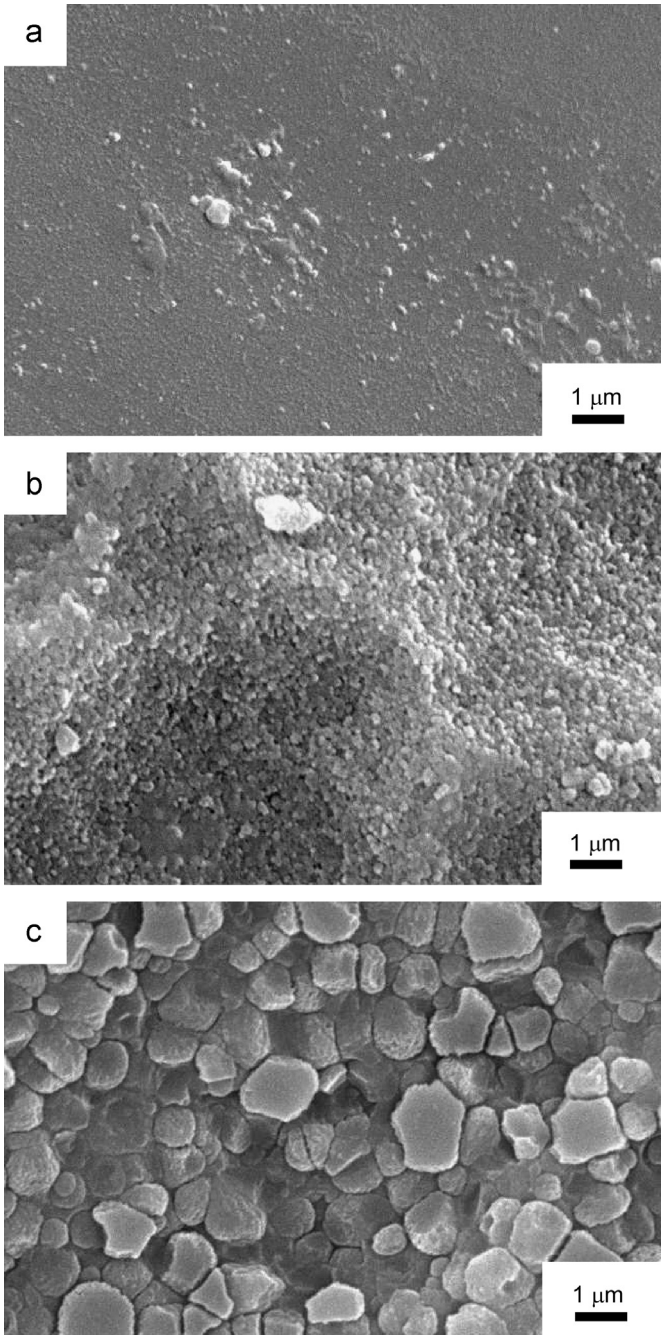


Fig. 6. Morphologies of La1 glass-ceramics annealed at different temperatures: (a) 740 °C, (b) 770 °C and (c) 840 °C.

100 nm. With increasing $La_2O_3$ content, the grain size increased, which indicated that the $La_2O_3$ addition enhanced the grain growth of the glass-ceramics.

The infrared spectra of the glass-ceramics are plotted in Fig. 9. There were mainly two absorption envelopes centered on 433 and 1078 $cm^{-1}$. Low-frequency bands (400–500 $cm^{-1}$) were generally attributed to the vibrations of O–Si–O bonds. The vibrations of Si–O–Si and Si–O–Al bonds were observed in the region of 950–1200 $cm^{-1}$. The center and intensity of all peaks seemed to be independent on the $La_2O_3$ content, which indicated that the $La^{3+}$ ions acted as network modifier.

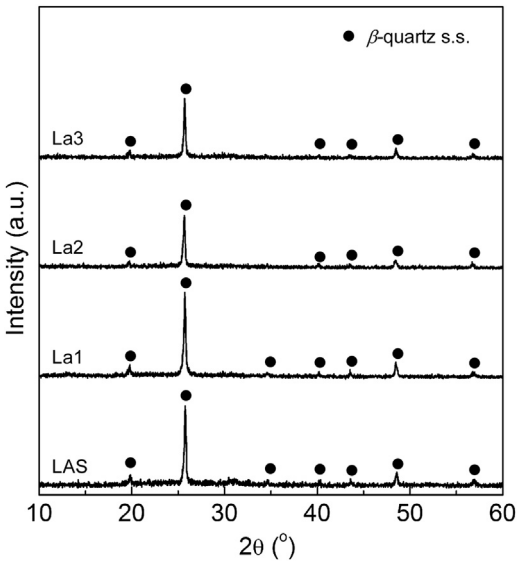


Fig. 7. XRD patterns of La-doped LAS glass-ceramics with different $La_2O_3$ contents.

The values of flexural strength for the La-doped LAS glass-ceramics are listed in Table 2, and Table 3 lists their thermal expansion coefficient. With increasing $La_2O_3$ content, the flexural strength decreased, and the thermal expansion coefficient increased. Usually, the physical properties of the glass-ceramics depend on the microstructures and their major crystal phases. As the $La_2O_3$ addition was introduced to the LAS glass-ceramics, the major phases did not change (as shown in Fig. 7), and the microstructures were obviously affected (as shown in Fig. 8). These results indicate that the mechanical properties of the La-doped glass-ceramics were mainly influenced by their microstructures. There are three classes of components for oxide glasses: network formers, intermediates and modifiers. For $La^{3+}$ ions, due to the large ionic radius (106.1 pm) and large coordinate number ($>6$), it plays a role of network modifier in the glass altering their network structure. The rare-earth ions in the glass were compensated by nearby non-bridging oxygen ions. The presence of non-bridging oxygen ions lowered the relative number of strong bonds in the glass and disrupted the network, which induced to decrease the crystallization of the glass-ceramics. The $La_2O_3$ addition enhances the grain growth of the glass-ceramics. With increasing the $La_2O_3$ content, the grain size increased. However, the glass-ceramics were easily broken along the grain boundaries, and the larger grain boundaries induced to decrease the flexural strength. At the same time, due to the large polarization of $La^{3+}$ ions, the bond strength of Si–O and Si–O–Si was weakened, which also resulted in the decrease of the flexural strength and the increase of the thermal expansion coefficient.

## 4. Conclusions

The La-doped LAS glass-ceramics were prepared by the solid phase reaction. The crystallization temperature of LAS glass-ceramics decreased due to the $La_2O_3$ addition. For the

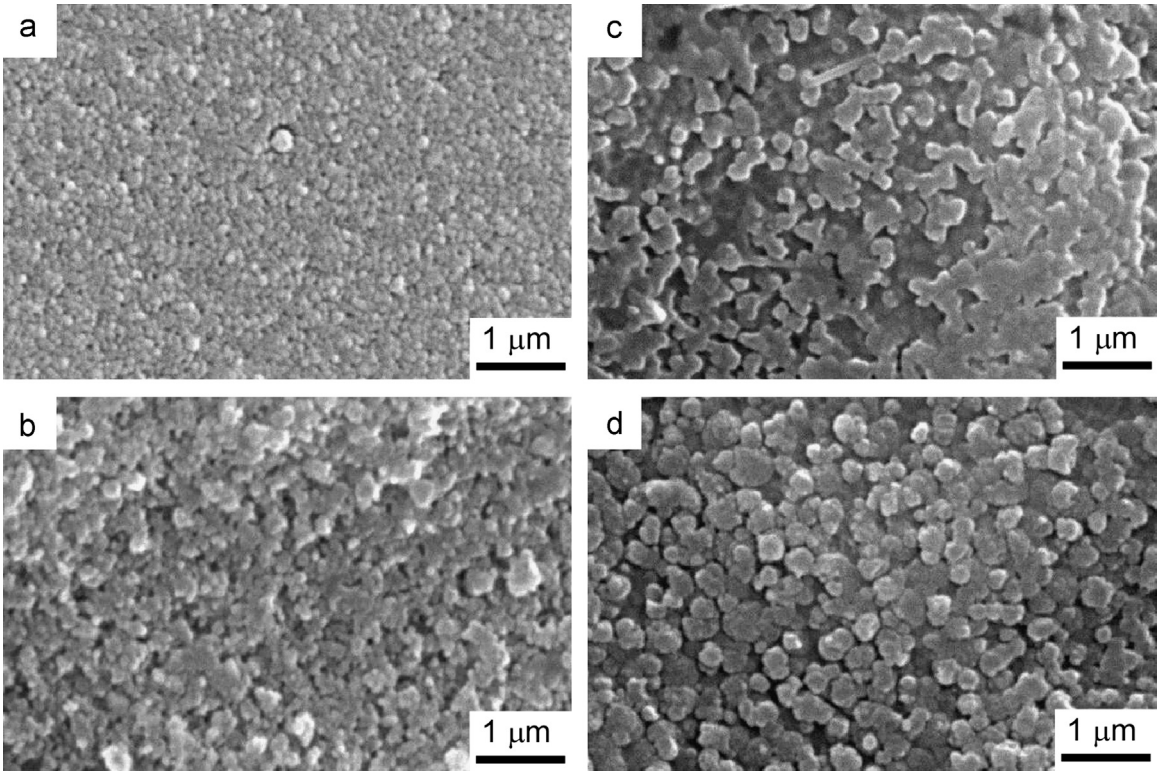


Fig. 8. Morphologies of La-doped LAS glass-ceramics: (a) LAS, (b) La1, (c) La2 and (d) La3.

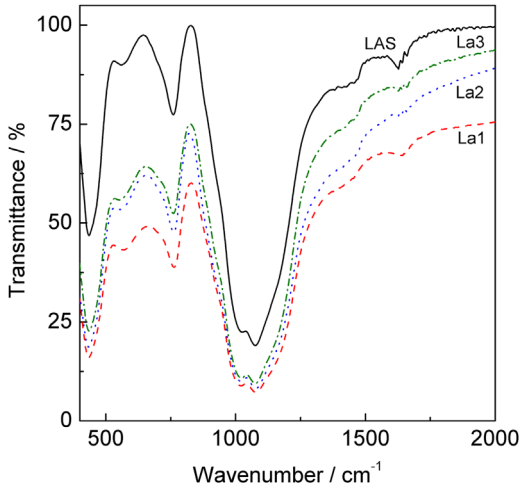


Fig. 9. Infrared spectra of the La-doped LAS glass-ceramics.

Table 2
The flexural strength of La-doped LAS glass-ceramics.

| | LAS | La1 | La2 | La3 |
|---|---|---|---|---|
| Flexural strength (MPa) | 105.66 | 90.55 | 68.20 | 47.90 |

La-doped LAS glass, the $\beta$-quartz s.s. was initially formed, and then the $\beta$-quartz s.s. transformed to $\beta$-spodumene at higher temperature. The $La_2O_3$ addition played a role of network modifier in the LAS glass altering their network structure. With increasing the $La_2O_3$ content, the flexural strength decreased, and the thermal expansion coefficient increased.

Table 3
The coefficient of thermal expansion of the La-doped glass-ceramics in the temperature ranging from 20 to 400 °C.

| | LAS | La1 | La2 | La3 |
|---|---|---|---|---|
| Thermal expansion coefficient ( $\times 10^{-7}$ °C$^{-1}$) | 0.84 | 2.37 | 14.54 | 22.81 |

## References

[1] A. Kidari, C. Mercier, A. Leriche, B. Revel, M.J. Pomeroy, S. Hampshire, Synthesis and structure of Na–Li–Si–Al–P–O–N glasses prepared by melt nitridation using $NH_3$, Materials Letters 84 (2012) 38–40.

[2] M. Dressler, B. Rudinger, J. Deubener, An *in-situ* high-temperature X-ray diffraction study of early-stage crystallization in lithium alumosilicate glass-ceramics, Journal of the American Ceramic Society 94 (2011) 1421–1426.

[3] R. Wurth, M.J. Pascual, G.C. Mather, A. Pablos-Martin, F. Munoz, A. Duran, G.J. Cuello, C. Russel, Crystallisation mechanism of a multicomponent lithium alumino–silicate glass, Materials Chemistry and Physics 134 (2012) 1001–1006.

[4] A.A. Dymnikov, O.S. Dymshits, A.A. Zhilin, V.A. Savostjanov, T.I. Chuvaeva, The structure of luminescence centers of neodymium in glasses and transparent glass-ceramcics of the $Li_2O$–$Al_2O_3$–$SiO_2$ system, Journal of Non-Crystalline Solids 196 (1996) 67–72.

[5] R. Krsmanovic, S. Bals, G. Bertoni, G.V. Tendeloo, Structural characterization of Er-doped $Li_2O$–$Al_2O_3$–$SiO_2$ glass ceramics, Optical Materials 30 (2008) 1183–1188.
[6] M. Mortier, A. Monteville, G. Patriarche, G. Maze, F. Auzel, New progresses in transparent rare-earth doped glass-ceramics, Optical Materials 16 (2001) 255–267.
[7] P. Riello, S. Bucella, L. Zamengo, U. Anselmi-Tamburini, R. Francini, S. Pietrantoni, Z.A. Munir, L.A.S. Erbium-doped, glass ceramics prepared by spark plasma sintering, Journal of the European Ceramic Society 26 (2006) 3301–3306.
[8] J.J. Shyu, C.S. Hwang, Effects of $Y_2O_3$ and $La_2O_3$ addition on the crystallization of $Li_2O \cdot Al_2O_3 \cdot 4SiO_2$ glass-ceramic, Journal of Materials Science 31 (1996) 2631–2639.
[9] W. Zheng, J. Cheng, L. Tang, J. Quan, X. Cao, Effect of $Y_2O_3$ addition on viscosity and crystallization of the lithium aluminosilicate glasses, Thermochimica Acta 456 (2007) 69–74.
[10] A. Hu, K. Liang, F. Zhou, G. Wang, F. Peng, Phase transformations of $Li_2O$–$Al_2O_3$–$SiO_2$ glasses with $CeO_2$ addition, Ceramics International 31 (2005) 11–14.